

RG Mapping: Learning Compact and Structured 2D Line Maps of Indoor Environments

Derik Schröter¹, Michael Beetz¹, Jens-Steffen Gutmann²

¹ Munich University of Technology ² Sony Corporation, Tokyo, Japan, Dig. Creatures Lab.
Boltzmannstr. 3, 85748 Garching b. München, Germany

Abstract—In this paper we present **Region and Gateway (RG) mapping**, a novel approach to laser-based 2D line mapping of indoor environments. RG mapping is capable of acquiring very compact, structured, and semantically annotated maps. We present and empirically analyze the method based on map acquisition experiments with autonomous mobile robots. The experiments show that RG mapping drastically compresses the data contained in line scan maps without substantial loss of accuracy.

I. INTRODUCTION

Many autonomous mobile service robots use maps, models of their environments, as resources to perform their tasks more reliably and efficiently. The need for quick deployment requires the robots to autonomously acquire maps of their new operating environments.

A number of software systems and algorithms for the acquisition of environment maps of office buildings, museums, and other indoor environments have been developed [2], [15], [5]. Robots acting in indoor environments most commonly use range sensors for acquiring maps of their environments and localizing themselves using the maps [2]. While most recent mapping algorithms have been designed to acquire very accurate maps [8], [5], [13], [11], [9], little attention has been paid to extend these algorithms to acquire additional information about the environment or make the representation compact.¹ Information that makes environment maps more informative for service robot applications include representations of the environment structure, object hypotheses, and characteristics of substructures that affect navigation and exploration.

In this paper we describe **RG** mapping (range data based **Region and Gateway** mapping) an autonomous robot mapping system that is capable of acquiring **RG** maps (**Region and Gateway** maps). RG maps are very compact, structured, and semantically annotated maps.

The key components of the RG mapping system are the Local Registration and Global Correlation (LRGC) method [8] which is an accurate range sensor based 2D map acquisition system, and additional sophisticated sensor data interpretation modules presented in this paper.

RG maps represent environments as a set of regions connected by gateways.² Regions are described compactly using a set of line segments and classified into different categories such as “office-like” or “hallway-like” regions. Regions provide additional information including main axes and measures of accu-

racy. The gateways represent transitions between regions.

This paper makes several important technical contributions to the area of robot map acquisition. First, we propose a new line merging algorithm that infers compact yet accurate line segment-based geometric descriptions. Because these 2D-line maps describe areas as a small number of line segments they yield smaller search spaces for generating object hypotheses. Second, we present a region-based interpretation of sensor data. Region-based sensor data interpretation can achieve more accurate line segment maps because they prevent the merging of lines that cannot result from the same objects parts, such as observations of opposite sides of a wall. The region based analysis of sensor data produces additional information such as main axes that inform adaptive exploration strategies that minimize odometric errors. Third, we propose an adaptive map acquisition method, in which the parameterization of sensor data interpretation algorithms are optimized for the characteristics of the respective regions. The adequacy of a parameterization is measured by assessing the distance between a line scan that is back projected from the map obtained with the parameterization and the original range scan.

The remainder of the paper is organized as follows. Section II describes our map representation. Section III outlines the map acquisition process. Specific sensor interpretation techniques are detailed in section 4. Section V empirically evaluates aspects of RG mapping. We end with perspectives for future work and our conclusions.

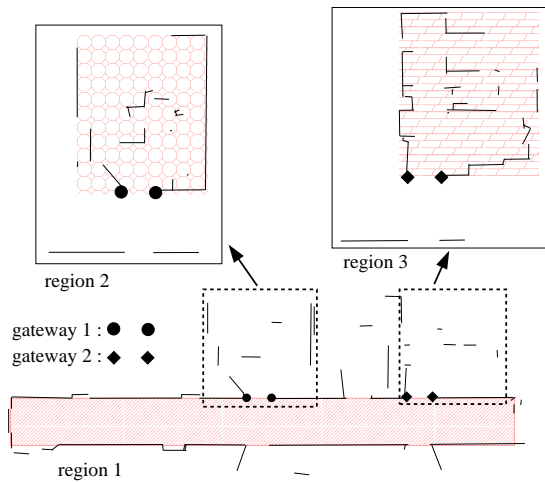
II. MAP REPRESENTATION

Buildings, in particular office buildings, are designed to be functional, well-priced, and efficient. Therefore buildings share salient design characteristics. They are structured into rooms that can be entered through doorways, and connected by hallways. In this section we propose RG maps as a means of representing such structures.

Before we lay out our basic representational concepts let us first consider figure 1 to get an intuition of how office environments are represented as an RG map. The map shows three regions: region 1 to 3 connected by two gateways of type narrow passage. The regions are visualized through their geometric description, a set of line segments. Bounding boxes of the regions, the smallest rectangle containing all possible robot positions in the region, are indicated through the background fill patterns. Among other things, the geometric description is used to predict the laser scan that the robot should receive at a given location within the region. Note that the geometric description contains lines that are outside the region’s bounding box. This

¹Notable exceptions include Thrun [12] who extracts topological from grid maps to speed up navigation planning. Tomatis et al. [14] propose a very compact representation using sets of infinite lines.

²Such maps have been already proposed in the context of cognitive maps [3] and topological maps [10].



	# lines	class	axis 1	axis 2	accuracy
region 1	58	CDMA	90	0	380.83 mm
region 2	24	TOMA	0	90	541.27 mm
region 3	38	TOMA	0	90	518.05 mm

Fig. 1. Map of our department floor, 781 laser scans, 124489 points

is because these lines can be seen through the gateway and used for robot self-localization.

RG maps are tuples $\langle R, G \rangle$, where R denotes a set of regions and G is a set of gateways that represent the possible transitions between regions. A region has a class label, a compact geometric description (for now we use 2D-lines), a bounding box, one or two main axes, a list of adjacent gateways, and a set of object hypotheses.

Currently, we use the following class labels for regions: closed and open regions with a distinct main axis (CDMA- and ODMA-regions), regions with two orthogonal main axes (TOMA-regions), and cluttered characteristic (CC-regions). Typically, hallways are classified as CDMA- or ODMA-regions and offices as TOMA- or CC-regions. Additional region classes can be defined.

The geometric description of a region consists of a set of 2D lines that best match the received laser range data and odometry readings. The lines of a region produce a very compact and accurate line based local 2D-map. Regions are associated with a measure of accuracy that specifies how accurately the geometric description reflects the sensor data obtained in this region. Region representations also comprise a set of object hypotheses, which are subsets of 2D lines that might belong to the same object in 3D. This will be used as an initialization for camera based object recognition in future work.

The second key component of our map representation are gateways. Gateways represent transitions from one region to another. In indoor environments several types can be distinguished, e.g. hallway T/L/X-junctions as well as small passages and changes from a rather narrow hallway into an open room, e.g. a lobby. Gateways are specified by a class label, adjacent regions, traversal directions, crossing-points and gateway-points that can be used for detecting when a gateway is entered and left. A number of researchers including Kortenkamp [10], Youngblood [15], Chown [4] and Schultz [1] have proposed gateways as first class objects in map representations.

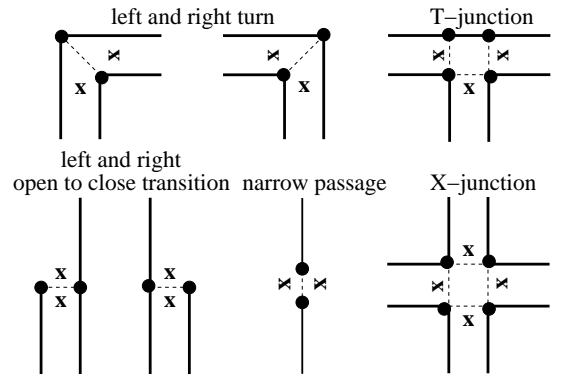


Fig. 2. gateways with crossing-points (X) and gateway-points (bullet)

III. MAP BUILDING

After having described RG maps, we will now turn to the question of how they can be acquired.

Figure 3 depicts the interaction of the RG mapping system with the robot. Currently, we run the system on an RWI B21 mobile robot equipped with a 180 degree laser range finder that is mounted horizontally at a height of about forty centimeters facing to the front. The mapping system continually receives sensor data from the laser range finder and the robot's odometry. The mapping system issues low-level commands to the robot's drive in order to navigate the robot through the environment.

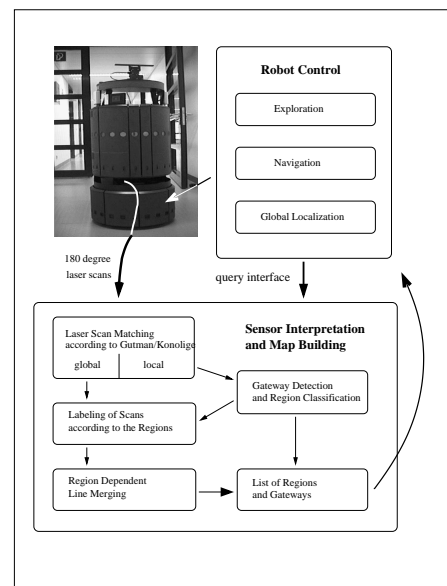


Fig. 3. System Overview

The mapping system itself consists of two main modules: the robot control (RC) and the sensor interpretation/map building module (SIMB). The RC module essentially computes where the robot should go next and performs the necessary navigation tasks. To do so the SIMB module provides the RC module with a representation of the region the robot is in and the gateways that the robot can pass in order to leave the current region. In addition, the RC module accesses the environment map through a query interface in order to determine which area of the environment it should explore next.

The sensor interpretation and map building proceeds as fol-

lows. First, a laser scan that is provided by the sensor is matched with the map built so far and then the scan is described more compactly through a sequence of line segments. The last k line scans are then used by the gateway detection and region classification module in order to detect when the robot is entering new regions and to classify the region that the robot is currently in. In a concurrent step the scan is associated with the region that the robot is currently in. Finally, the new line scan is merged with the existing representation of the region in order to improve the accuracy and completeness of the region representation and make the representation more compact. The output of this step updates the environment map.

The map is not only used for task achievement but also for achieving a better exploration behaviour. Once we have determined certain characteristics for a region, we can adapt the exploration method accordingly, mainly to avoid rotation, which is known to cause the most inaccuracies in odometry. For example, in a hallway (CDMA-region) one would first drive along the main axis and later when this region is fully explored enter other regions. In an “office-like” region (TOMA/CC-region), it is not appropriate to follow a certain main axis, because this axis might be difficult to determine due to clutter. Instead one would rather go to distinctive places to maximize the information gain while minimizing odometric errors. Another alternative is to generate a map for an office as fast as possible, and then restart this process with the knowledge from the first run, hence with optimized routes.

Furthermore, the map initializes and supports the generation of 3D object hypothesis, which works as follows. First, we extract the room structure from the 2D-line set describing the region. That means estimating the position of the walls, which is similar to the before mentioned bounding rectangle for a region. The lines included in that rectangle are grouped into object hypotheses. For example, an office closet would have a rectangular outline. Such a description provides clues concerning depth irregularities, which can be correlated with 3D-data derived from stereo-vision. In this special case, we could assume a cube in 3D and search for the regarding vertical and horizontal lines as well. Together this means that the vision based 3D mapping process is initialized with the 2D information retrieved from laser data. Another example is a poster on a plain wall, e.g. in a hallway. First we find the rectangle describing the poster and measure the pose of the corners in global coordinates, then we relate those coordinates to lines in the 2D-description. If there are matches they are most likely due to the wall measured with the laser range finder. Thus we can correct the pose of the poster according to the laser measurements. In other words, we would certainly not observe the poster without vision, but since depth information obtained using stereo-vision is not as precise as data acquired using the laser range finder, we use the latter to increase accuracy of the 3D-landmarks.

IV. ACQUIRING COMPACT MAPS

Let us now turn to the issues of making maps compact, adjusting the mapping parameterization in region specific ways, and structuring environments into regions.

A. Laser Scan Matching

The first step in the sensor interpretation task is to match a scan s obtained by the laser range finder into a local map m . The scan matching routine is given a local map m and a range scan s and uses a random variable l whose range is the set of all possible poses (position and orientation of the sensing device) in the local map. The scan matching routine computes a probability distribution $P(l|m, s)$ over the possible poses given the local map m and the scan s . In RG mapping we use Gutmann and Konolige’s Local Registration/Global Correlation (LRGC) algorithm [8] to perform this step.

Having computed the probability distribution over the possible poses we take the global maximum of the distribution (if its probability exceeds a given threshold) to be the real pose from where the reading was taken. In order to reduce the complexity of the subsequent sensor interpretation steps we convert the scan consisting of a sequence of measure points into a sequence of line segments using an algorithm proposed by Gutmann in [6].

B. Line Merging Algorithm

The next sensor interpretation step is the update of the line segment representation of the current region. The computational task is: given the geometric description (gd) of the region (a set of line segments) and a new line scan produced by the laser scan matching, update the geometric description (gd) such that it also reflects the evidence contained in the new line scan. This computational task is performed by the line merging algorithm, which compares each line with each other line (from the total set of line-scans describing a region), and determines if they should be merged. In the remainder of this section we will explain when and how lines are merged.

A distance measure for line segments in 2D line maps.

When should RG mapping merge a line in the laser scan with a line in the local geometric description? We define a fast 2D distance measure for line segments to answer this question.

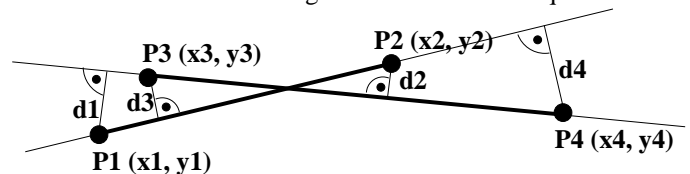


Fig. 4. Distance measure between line segments.

Consider figure 4 to get an intuition of what the distance measure should do. The main task is the identification of the same lines in the current and the previous scans. This is complicated by the facts that the lines might be translated and rotated due to noise in the odometric and range data. Therefore the distance measure should recognize lines that are identical even in the light of inaccurate measurements. On the other hand, laser readings generated by small objects such as the legs of chairs can often not be distinguished from false measurements. The trade-off between these conflicting objectives in line merging are determined by the algorithm’s parameterization.

Before we describe the algorithm in more detail let us first make the following definitions. Let l^1 and l^2 be two line segments given by their end points (P_1, P_2) and (P_3, P_4) , respectively. The distance of an endpoint to the opposing line is given

by the perpendicular, the shortest distance to that line, as shown in Figure 4.

An overlap o^P of point $P(x, y)$ regarding line $l(x_s, y_s, x_e, y_e)$ is defined to be equal to one if:

$$[(x > x_s) \text{ AND } (x < x_e)] \text{ OR } [(x < x_s) \text{ AND } (x > x_e)]$$

Otherwise o^P is zero. Hence for each point P_i we get the tuple (d_i, o_i^P) . Considering the end points we can distinguish three overlapping cases (o^l) for two given lines - no overlap, simple overlap and complete overlap as shown in Figure 5. Note that $\sum o_i^P$ can only be zero or two.

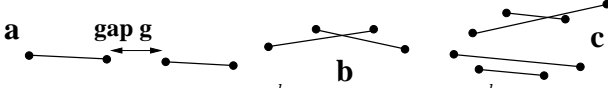


Fig. 5. overlap types: no overlap, $o^l=0$ (a), simple overlap $o^l = 1$ (b), complete overlap $o^l = 2$ (c)

The final distance measure between the two lines and the line overlap mode are determined by a simple and fast algorithm as shown below. A distance threshold defines whether or not the lines are close enough to be merged. In this paper we take values between 50 to 100 millimeter. But as will be shown later the optimal threshold also depends on the characteristics of the environment.

$$(d, o^l) = \begin{cases} (res_1, 0) : (res_1 < res_2) \text{ AND } (\sum o_i^P = 0) \\ (res_2, 0) : (res_1 > res_2) \text{ AND } (\sum o_i^P = 0) \\ (res_1, 1) : (res_1 < res_2) \text{ AND } (\sum o_i^P = 2) \\ \quad \text{AND } (o_1^P + o_2^P \neq 2) \text{ AND } (o_3^P + o_4^P \neq 2) \\ (res_2, 1) : (res_1 > res_2) \text{ AND } (\sum o_i^P = 2) \\ \quad \text{AND } (o_1^P + o_2^P \neq 2) \text{ AND } (o_3^P + o_4^P \neq 2) \\ (res_1, 2) : o_1^P + o_2^P = 2 \\ (res_2, 2) : o_3^P + o_4^P = 2 \end{cases}$$

$$\text{where } res_1 = \frac{d_1 + d_2}{2} \text{ and } res_2 = \frac{d_3 + d_4}{2}$$

Updating Lines. After determining whether two lines should be merged an iterative line merging algorithm calculates the resulting line using a fairly simple, online linear regression. For computational purposes the line comprises not only start (x_1, y_1) and end point (x_2, y_2) but also its weighted first and second order moments. The index i refers to the lines which are to be merged into the resulting line, and it is obvious that those calculations can be done iteratively whenever a new line has to be added.

$$\begin{aligned} sum_X &= \sum length_i * (x_1^i + x_2^i) \\ sum_Y &= \sum length_i * (y_1^i + y_2^i) \\ sum_W &= \sum 2.0 * length_i \\ sum_{XY} &= \sum length_i * (x_1^i * y_1^i + x_2^i * y_2^i) \end{aligned}$$

For $slope \leq 45$ degree:

$$sum_{XX} = \sum length_i * ((x_1^i)^2 + (x_2^i)^2)$$

and for $slope > 45$ degree:

$$sum_{YY} = \sum length_i * ((y_1^i)^2 + (y_2^i)^2)$$

Afterwards we determine the resulting line in the case that $slope \leq 45$ degree according to:

$$slope = \frac{sum_{XY} * sum_W - sum_X * sum_Y}{sum_W * sum_{XX} - (sum_X)^2}$$

$$offset = \frac{sum_{XX} * sum_Y - sum_X * sum_{XY}}{sum_W * sum_{XX} - (sum_X)^2}$$

And analogous for $slope > 45$ degree by simply replacing sum_{XX} with sum_{YY} .

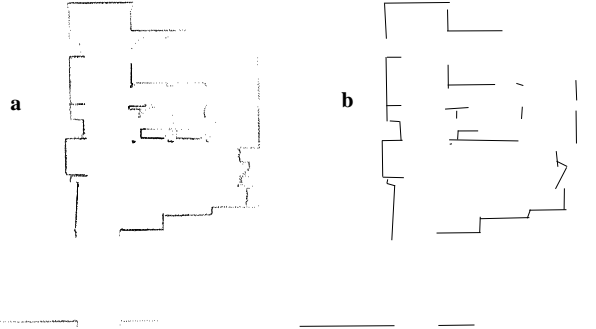


Fig. 6. (a) original data for a region comprising 30 scans and 5042 points, (b) line merged version, the same region is represented by 38 lines

C. Parameterization/Adaptation

When developing map representations that can mirror building structures there are two problems to consider. First, not all indoor environments share these structures. Second, even if they do it might not be possible to infer this structure from the range data. On the other hand, maps representing such structures provide important information for many service tasks. The accuracy of the acquired maps can be further increased by utilizing such structures to bias map learning algorithms. In this section we discuss the parameters of the scan matching and the line merging algorithms that correlate with these aspects.

The line merging algorithm can be primarily parameterized through the so-called minimal line segment μ , distance/length ratio ρ , and the line gap factors γ . Lines shorter than μ are ignored. If the distance/length ratio, defined as the ratio between the distance measure and the length of the line to be merged exceeds ρ then the line is disregarded. This is the case when trying to merge a small line which is almost rectangular to the reference line (because of noise). Finally, the gap threshold γ defines when two lines should be merged even if they do not overlap at all ($o^l = 0$). Our experience suggested values of 0.1 to 0.4 for the length factor and about 200 millimeter for the gap threshold.

Likewise in the laser scan matching routine we have parameters that include the maximal distance of measure points from a given cluster, the maximal distance of a point from a line, the maximal tolerated variance of points associated with a line, the minimum number of point measurements that constitute a line segment, and the minimum length of a line.

The parameterization can be chosen to minimize the number of lines in the map. In this case we would use a strong parameterization, i.e. small tolerated variance, high number of points supporting a line etc., in order to suppress small lines generated from noisy data, e.g. in hallways. On the other other hand we might loose important details in cluttered environments. This is particularly true for table-legs, which are represented in the laser scans by only a few points. Hence, we would rather generate more lines here, in order to generate an accurate map. That means, the parameterization is a trade-off between compactness and accuracy, and depends on the characteristics of the environment. Currently, we use several heuristics to accomplish this

task. But it is still one of the main issues in ongoing research to develop a more general approach for this adaptation.

The accuracy of the 2D-line maps is determined using the distance measure $acc(s_i)^2 = \frac{1}{N} \sum_{k=0}^N (d_k^o - d_k^m)^2$, where s_i^o denotes the original scan containing N distance measures d , and s_i^m the reproduced scan based on the line map. If there is no distance measure in the reproduced scan due to a missing line, a penalty value p is added instead. Hence, distance measures which are not represented in the map will not be overestimated, which could be the case if we would simply set this measure to zero, or allow for large (unrelated) distance readings. The resulting accuracy for a region R containing M scans is then: $acc(R)^2 = \frac{1}{M} \sum_{i=0}^M acc(s_i)^2$. Section 5 shows the application of the distance measure.

D. Structuring the Maps

When building RG maps, the robots must be aware of when they enter and leave regions. To recognize the entering and leaving of regions the map structuring routine employs a *finite state automaton* that records the respective state of the mapping process: in-ODMA-region, in-CDMA-region, in-TOMA-region, in-CC-region, in-unclassified-region, and entering-unknown-region. The second component is the *gateway detector*. In the remainder of the section we explain (1) how we detect gateways and thereby infer regions and (2) how we classify the regions.

Detecting Gateways. Gateway hypotheses are generated based on a single scan as outlined before. Our current prototypical implementation simply (1) computes the the closest obstacles left and right; (2) tests certain distance, free space, and angle properties wrt. these obstacles, and (3) tests the hypothesis using an artificial neural network trained with typical gateway scans and cluttered surrounding scans. Since doorways and certain constellations of furnitures cannot be distinguished based on laser scans we currently work on adding cameras to the detection process. The detection of T/L/X-junction gateways operates similarly using different feature descriptions.

Classifying Regions. To classify regions RG mapping uses a set of features which are based on a line angle histogram and on different measures of the free space. The line angle histogram is computed by summing up the length of lines with equal or similar slope, scaling it, and shifting the maximum to the center.

The classification is performed by an artificial neural network that has been trained with different characteristic histograms, i.e. a Gauss distribution with maximum 1.0 (single main peak), two Gauss distributions (one is maximum 1.0, the other from a lower level up to one) with an angle difference of 90 degrees and finally simply noise between a certain lower value and 1.0. Extra noise of different amplitude has been added to all synthetic histograms. The chosen distributions refer to ODMA/CDMA-, TOMA- and CC-regions, respectively.

V. EXPERIMENTAL RESULTS

In this section, we empirically evaluate the different aspects of RG mapping: the compactness and accuracy of the resulting maps and the effects of parameter adjustment for the scan matching and line merging routines.



Fig. 7. RG map of our department floor at TUM IX.

Compactness. In the first series of experiments we empirically evaluate the reduction of the map size that is accomplished through RG mapping with respect to scan matching and scan matching with line extraction. Table I lists the results of RG mapping for several environments. *region 1*, *region 2* and *region 3* refer to figure 1 and are part of our department floor that is depicted in figure 7 and figure 8 shows the RG map generated from the Wean Hall data set, which is a de facto benchmark problem for laser-based map building.³ The right most table column shows the number of lines after merging, which constitute a substantial data compression (factor 7 to 17). The main advantage, however, is that the the reduction reduces the search space for object hypothesis generation, which scales with the number of line segments.

	# scans	# points	# lines	# RG lines
Wean Hall	942	56221	4013	503
GI Demo	111	19476	600	34
TUM IX	761	64451	3733	494
region 1	90	13903	409	58
region 2	35	6042	269	24
region 3	30	5042	256	38

TABLE I

REDUCTION OF COMPLEXITY FOR SEVERAL MAPS

Accuracy. Having achieved such a substantial data compression raises the question whether the compression yields substantial inaccuracies. In order to evaluate the accuracy of the RG maps we have performed two kinds of experiments. In the first one we show that based on RG maps the robot can determine its position very accurately.

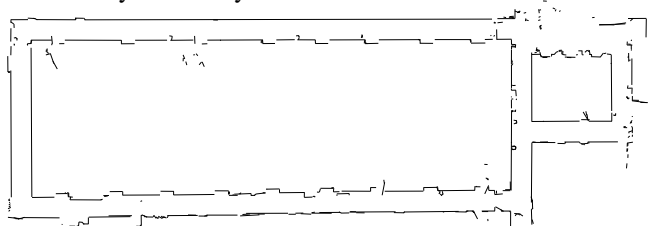


Fig. 8. RG map for the Wean Hall data set.

To do so we used the data that the maps were built to simulate a moving robot. We assumed the start position to be known. The localization matches the original range data with a scan calculated from the map at the same position. As a result we get an estimate for the current position, which we compare with the according aligned scan, that was actually part of the map building process before. In [7] it has been shown that the localization based on laser scans is very accurate/precise. Therefore we take it as ground truth. The results are summarized in table II.

We have also determined the accuracy by comparing how well the line segments match the scans they have been produced from

³The data set has been provided by Sebastian Thrun.

(all in mm)	δx	δy	$\delta \alpha$	d_{min}	d_{max}
GI Demo	-1.6 ± 24.4	0.84 ± 11.3	0.002 ± 0.01	0.4	27
TUMIX	-5.2 ± 83.2	1.3 ± 88.9	-0.003 ± 0.02	0.29	653.8

TABLE II
LOCALIZATION ACCURACY

using the distance measure we have defined before. The average inaccuracy for the Ween Hall data set shown in figure 8 map is about 429 mm.

Another accuracy gain is shown in the map of figure 9. Here region-based mapping is able to distinguish between two sides of the wall even though the wall has been only a couple of centimeters thick. We had similar effects as we built maps of our office floor. We have also made experiments with different parameterizations of the scan line matching and line merging algorithms that show that the accuracy of RG maps can be substantially increased by choosing the parameterizations that minimize the error with respect to our distance measure.

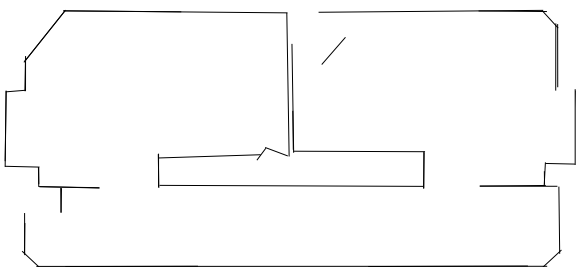


Fig. 9. RG map for the GI demo.

VI. CONCLUSIONS

In this paper we have presented **Region and Gateway (RG)** mapping, a novel approach to laser-based 2D line mapping of indoor environments. We have shown in experiments on autonomous robots that RG mapping is capable of acquiring very compact, accurate, and region-structured 2D line maps. In our overall research agenda RG maps are an important milestone in our development of a vision-based 3D mapping system that computes maps with 3D object hypotheses. Besides the development of a vision-based 3D object hypothesis generation system we intend to develop better exploration strategies and deal with dynamic objects such as doors.

REFERENCES

- [1] W. Adams, D. Perzanowski, and A.C. Schultz. Learning, Storage, and Use of Spatial Information in a Robotics Domain. In *Proc. of the ICML 2000 Workshop on Machine Learning of Spatial Language*, pages 23–27. Stanford University: AAAI Press.
- [2] W. Burgard, A.B. Cremers, D. Fox, D. Hähnel, G. Lakemeyer, D. Schulz, W. Steiner, and S. Thrun. Experiences with an interactive museum tour-guide robot. *Artificial Intelligence*, 114(1-2), 2000.
- [3] Eric Chown. Making predictions in an uncertain world: Environmental structure and cognitive maps. *Adaptive Behaviour*, pages 1–17, 1999b.
- [4] Eric Chown. Gateways: An approach to parsing spatial domains. In *ICML 2000 Workshop on Machine Learning of Spatial Knowledge*, 2000.
- [5] T. Duckett, S. Marsland, and J. Shapiro. Simultaneous Localization and Mapping - a new algorithm for a compass-equipped mobile robot. In *Proc. of the IJCAI, Workshop on Reasoning with Uncertainty in Robotics*, 2001.
- [6] J.-S. Gutmann. Robuste Navigation autonomer mobiler Systeme (in German). Akademische Verlagsgesellschaft Aka, Berlin, 2000. Doctoral Thesis University of Freiburg.
- [7] J.-S. Gutmann, W. Burgard, D. Fox, and K. Konolige. An experimental comparison of localization methods. In *Proc. of the IEEE/RSJ International Conference on Intelligent Robots and Systems (IROS)*, 1998.

- [8] J.-S. Gutmann and K. Konolige. Incremental mapping of large cyclic environments. In *Proc. of the IEEE International Symposium on Computational Intelligence in Robotics and Automation (CIRA)*, 2000.
- [9] D. Haehnel, W. Burgard, and S. Thrun. Learning Compact 3D Models of Indoor and Outdoor Environments with a Mobile Robot. In *The fourth European workshop on advanced mobile robots (EUROBOT)*, 2001.
- [10] David Kortenkamp. *Cognitive Maps for mobile robots: A representation for mapping and navigation*. PhD thesis, University of Michigan, 1993.
- [11] Y. Liu, R. Emery, D. Chakrabarti, W. Burgard, and S. Thrun. Using EM to learn 3D models with mobile robots. In *Proc. of the International Conference on Machine Learning (ICML)*, 2001.
- [12] S. Thrun and A. Bcken. Integrating grid-based and topological maps for mobile robot navigation. In *Proceedings of the AAAI Thirteenth National Conference on Artificial Intelligence*.
- [13] S. Thrun, J.-S. Gutmann, D. Fox, W. Burgard, and B. Kuipers. Integrating topological and metric maps for mobile robot navigation: A statistical approach. In *Proc. of the AAAI Fifteenth National Conference on Artificial Intelligence*, 1998.
- [14] N. Tomatis, I. Nourbakhsh, and R. Siegwart. Simultaneous localization and map building: A global topological model with local metric maps. In *Proceedings of the IEEE/RSJ International Conference on Intelligent Robots and Systems (IROS 2001)*, 2001.
- [15] G.M. Youngblood, L.B. Holder, and D.J. Cook. A Framework for Autonomous Mobile Robot Exploration and Map Learning through the use of Place-Centric Occupancy Grids. In *Proc. of the Machine Learning Workshop on Learning From Spatial Information*, 2000.